Determination of electronic band structure of quaternary ferromagnetic $Ga_{0.97-x}Mn_{0.03}Cr_xAs$ epitaxial layers

Omer Donmez[1,*], Mustafa Gunes[2], Mohamed Henini[3] and Ayse Erol[1]

[1]*Department of Physics, Faculty of Science, Istanbul University, Vezneciler, 34134, Istanbul, Turkiye*
[2]*Department of Materials Engineering, Faculty of Engineering, Adana Alparslan Turkes Science and Technology University, 01250, Adana, Turkiye*
[3]*School of Physics and Astronomy, University of Nottingham, Nottingham NG7 2RD, United Kingdom*

**E-mail: omerdonmez@istanbul.edu.tr*

Abstract: In this study, the optical properties of $Ga_{0.97-x}Mn_{0.03}Cr_xAs$ thin films with various Cr concentrations are investigated using photomodulated reflectance (PR) spectroscopy at room temperature. PR spectra were analyzed with the third derivative functional form (TDFF) signal's line shape. Analysis of the TDFF shows that the fundamental bandgap of $Ga_{0.97-x}Mn_{0.03}Cr_xAs$ alloys increases with Cr concentration. The bandgap of $Ga_{0.97-x}Mn_{0.03}Cr_xAs$ alloy is calculated using the valence band anti-crossing (VBAC) model. The fundamental and spin split-off band related optical transition of the induced defect is calculated by VBAC model. The interaction energy between localized Mn- energy level and valance band edge, which is experimentally determined as 0.7 eV is in agreement with the one found by the VBAC model.

Keywords: Magnetic semiconductor, GaMnCrAs, modulated Photoreflectance, Band Anti-Crossing model

INTRODUCTION

Functional magnetic semiconductors (MS) based on III-V alloys meet the requirement of the spintronic technology for the control of both the charge carriers and the spin degree of freedom of the carriers due to the native magnetic order together with semiconductor characteristics [1,2]. To exploit these fundamental features and develop advanced technological devices using MS, the magnetic properties should be observed at least at room temperature. Different kinds of III-V semiconductors doped or alloyed with transition metal (TM) such as GaMnAs, GaCrAs, GaCrN, and GaMnN, have been utilized for spintronic applications [3–7]. However, it has been witnessed

that there is great solubility problem of TM in semiconductors to incorporate large amount of TM in semiconductors [4–6,8]. Hence, many studies have focused on the GaMnAs alloys due to their high solubility in III-V semiconductors and the easy manipulation of their magnetic properties by means of optical and electrical methods [9–12]. However, the GaMnAs alloys have Mn-related defects that form an impurity band (IB) above the valence band (VB) [2,13] and the electronic band structure of GaMnAs can be understood with impurity band model or valence band anti-crossing model [14,15]. As far as we know, there is still not an established unique model to explain the electronic band structure of GaMnAs.

The formation of the impurity (band) has led to the exploration of different kinds of MS, such as GaCrAs and CrMnAs materials, with the aim to increase Curie temperature. It has been shown that GaCrAs has a great potential for super-magnetism, but this property is suppressed by precipitation of TM in the lattice [16,17]. Lutz-Kappelman theoretically showed that antiferromagnetism of CrMnAs reveals with Cr-Cr, Cr-Mn and MM-Mn interactions [18]. However, the combination of Mn and Cr atoms in GaAs is still very scarce in the literature.

In order to eliminate the obstacle to advance MS materials due to the formation of defect states and/or nanoclusters, several approaches have been explored [19,20]. One of the methods to overcome the formation of defects and clustering in TM in semiconductors is co-doping MS with acceptors and donors atoms where the repulsion between transition metals occurs [21–23]. Mahadevan et *al*. showed theoretically that isovalent doping of GaAs with transition impurities such as V, Cr, Mn and Fe result in the substitution of Ga host atoms. The substituted solute doping atoms repulse each other, while pair of them attract each other and generate defect states in the bandgap [24]. These behaviors may be controlled by optimizing the growth conditions. However, the effect of high density of co-doping and alloying with two or more TM is still unknown.

In this study, we investigate the effect of the incorporation of both Cr and Mn atoms in GaAs on the optical properties and electronic band structure of GaMnCrAs semiconductor. The optical properties of GaMnCrAs semiconductor are investigated using photomodulated reflectance (PR) spectroscopy. The optical transitions in PR spectra are analyzed with third derivative functional form (TDFF). The electronic band structure of the alloys is determined by considering the impurity band model with valence band anti-crossing (VBAC) model. The optical transition type is identified by comparing TDFF analysis and VBAC model results.

MATERIALS and METHODS

$Ga_{0.97-x}Mn_{0.03}Cr_xAs$ thin films with x =0.005, 0.07 and 0.18 were grown on (001) semi-insulating GaAs substrates by molecular beam epitaxy (MBE). A 20 nm GaAs buffer layer was grown at around 580 °C, which was followed by a 100 nm thick $Ga_{0.97-x}Mn_{0.03}Cr_xAs$ epitaxial films grown at 220 °C±10°C. Secondary ion mass spectroscopy (SIMS) was used to determine the Mn and Cr concentrations of the samples. The layer structure of the samples is shown in Table 1.

Table 1: A schematic diagram showing the layer structure of the samples investigated in this study

$Ga_{0.967-x}Mn_{0.03}Cr_xAs$ -Epitaxial film (~100nm)
GaAs-Buffer (20nm)
SI- GaAs-Substrate

PR measurements were conducted at room temperature. In the experimental setup, 514 nm Argon-Ion laser and 100 W halogen lamp were utilized as pump and probe sources, respectively. The pump light is modulated at 167 Hz. The quasi white light from 100W halogen lamp was dispersed by an 0.5 m Acton 2500i monochromator, and dispersed light was detected with Si and GaInAs photodiodes. The output of the detectors was monitored with a lock-in technique. The details of PR measurements can be found elsewhere [25–30].

PR spectra were analyzed by using low electric field TDFF given as [21,25–30]

$$\frac{\Delta R}{R} = \sum_n A_n e^{-i\theta_n}[E_n - E_{TDFF} + i\Gamma_n]^{-m_n} \quad (1)$$

where A, θ, E, E_{TDFF} and Γ are the amplitude, phase, photon energy, optical transition energy, and line broadening, respectively. The type of critical point, depending on the dimensionality of the structures, is represented as m_n and its value is 2.5 for epitaxial layers. Details for fitting procedures can be found in Refs [29,31–33].

RESULTS and DISCUSSION

Figure 1 shows the PR spectra of $Ga_{0.97-x}Mn_{0.03}Cr_xAs$ alloys (x=0.005, 0.07 and 0.18) with TDFF fitting results at room temperature. The TDFF simulated PR spectra well match the experimental PR spectra. The obtained results using TDFF method are given in Table 2. We observed a sharp signal for GaAs layer (buffer or substrate), which suppresses the optical transitions above the bandgap of the GaAs layer as seen in Figure 1. However, the optical transition energies (T) are slightly lower than the well-known GaAs bandgap energy value due to the low temperature growth of the samples. The suppressed optical transitions become more prominent with increasing Cr concentration in alloys. In addition, a PR signal at higher energy region at >1.4 eV is observed. The optical transition signal at higher energies has more noise as compared to the lower energy transitions around GaAs bandgap energies. The optical transition energies will be addressed by calculating the electronic band structures. It is worth noting that we did not observe Franz-Keldysh effect in PR spectra, which is indicative of compensation of ionized defects inside the quaternary alloys. Full width at half maximum (FWHM) of the optical transition energies increases with Cr composition, except for T1. The optical transition energies and the FWHM of the PR lines are tabulated in Table 2.

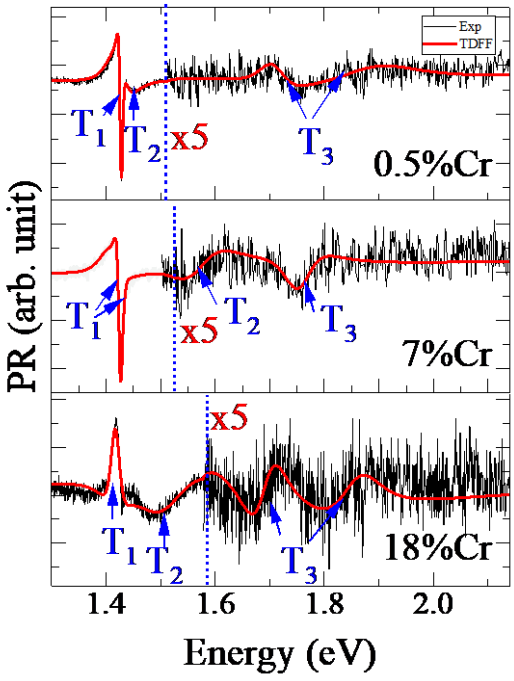

Figure 1: Experimental PR results (black solid line) with TDFF fitting of samples (red solid line) with a) 0.5% Cr, b) 7%Cr and 18% Cr, respectively. The data on the right-side of the blue dotted line are multiplied by a factor of 5 for clarity.

Table 2: Experimental optical transition energies (T) and FWHM values

%Cr	T_1 (eV)	FWHM (meV)	T_2 (eV)	FWHM (meV)	T_3 (eV)	FWHM (meV)
0.5	1.421	34	1.427	62	1.71/1.84	54/120
7	1.415/1.425	9/28	1.58	72	1.757	60
18	1.417	19	1.507	95	1.69/1.86	50/80

The formation of the electronic band structure of ferromagnetic Mn-doped GaAs is explained by Ruderman, Kittel, Kasuya, and Yosida (RKKY) model [21]. In this model, Mn atoms are located above the valence band (VB) and generate a shallow acceptor impurity band (IB). Chapler *et al.* reported that IB impurity band is still present up to 16% Mn concentration in $Ga_{1-x}Mn_xAs$ alloys [34]. Pela *et* al. theoretically showed that the position of the shallow impurity band with respect to VB depends on the Mn composition [35]. Alberi *et al*. modeled the electronic band structure of $GaMn_xAs_{1-x}$ alloys with VBAC model by considering the large differences of ionization energy, electron affinity, and radius between Mn and Ga atoms [15]. According to the VBAC model, the localized Mn atom state interacts with VB states, namely heavy hole (HH), light hole (LH), and spin split-off band (SO), where each band is split into two branches while the conduction band (CB) is not affected by the incorporation of Mn [15,25–27,30]. The HH band is divided into two new bands, one of them is an impurity band and the other is an optical band. This results in an upward shift of VB with regard to the top of the GaAs VB. The energies of the two new bands can be given by [15,25–27,30].

$$E_{\mp}(x)_{k=0} = 0.5\,[E_{VB}(x) + E_{Mn}^{VB} \mp \sqrt{(E_{VB}(x) - E_{Mn}^{VB})^2 + 4\,V_{Mn-VB}^2 x}\,] \qquad (2)$$

where x and E_{VB} are Mn atom composition and VB energy bands, namely HH, LH and SO bands, respectively. E_{Mn}^{VB} and V_{Mn-VB} are Mn atom energy level and the interactions between Mn-atom energy level and each VB edges, respectively. The electronic band structure of $Ga_{0.97}Mn_{0.3}As$ is calculated using VBAC model and shown in Figure 2a. In this model, $E_+(x)$ is the eigenvalue of IB band which is redshifted, while $E_-(x)$ is the eigenvalue of the top of VB which is blue shifted.

It is worth pointing out that the strain effect on the VB edges is not taken into account, hence, the eigenvalue of $E_{-}(x)$ in Eq. 2 is for both HH and LH at $k \approx 0$.

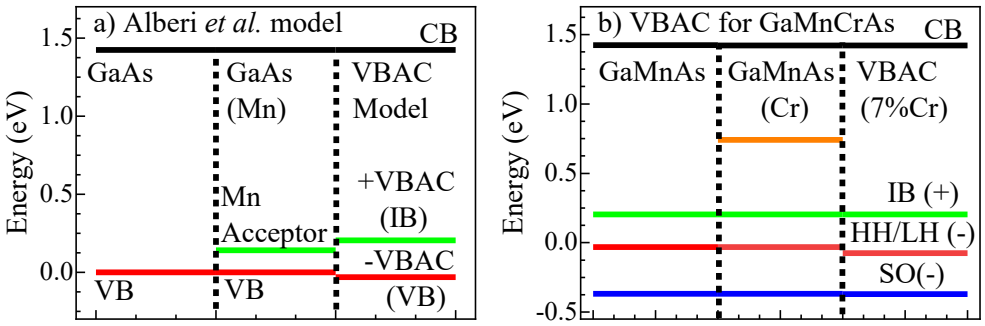

Figure 2: Formation of electronic band structure of ferromagnetic alloys for (a) $Ga_{0.97}Mn_{0.3}As$ and (b) $Ga_{0.90}Mn_{0.3}Cr_{0.07}As$. The parameter $V_{Mn/Cr-VB}$ is taken as 0.7 eV to obtain best fit for both $Ga_{0.97}Mn_{0.3}As$ and $Ga_{0.90}Mn_{0.3}Cr_{0.07}As$. +/- represent the roots of Equation 2 as being split energies.

In $Ga_{1-x-y}Mn_xCr_yAs$ alloys, Cr atoms substitute Ga atoms sites as in GaMnAs alloys and form GaMnCrAs alloys and the bandgap of the alloy can depend on the Cr composition in the alloy however, to the best of our knowledge, there is no reported value of the band gap and alloy composition dependence of the bandgap of $Ga_{1-x-y}Mn_xCr_yAs$ in the literature. It was shown that Cr atoms generate a donor impurity level in midgap of GaAs [36], which can be compensated with IB of Mn in $Ga_{1-x-y}Mn_xCr_yAs$.

Here, we exploit VBAC model to determine the band alignment of GaMnCrAs because there are large differences between ionization energy and electron affinity of Cr and Ga atoms. In the band alignment calculation, we consider the interaction between VB states and IB of Mn and Cr atoms. Firstly, the VBAC model is applied to $Ga_{0.97}Mn_{0.3}As$ alloy to find the energy levels by considering the interaction between VB/SO and IB of Mn level. Then, we calculate the energy state of $Ga_{0.97-y}Mn_{0.3}Cr_yAs$ alloys by taking into account the interaction between VB/SO and IB band of Mn and Cr atom levels. Considering all interactions between VBs and IBs, we have obtained several possible eigenvalues, but we show only some solutions of Eq. 2 in Figure 2b because optical transitions occur among them.

Figure 3 shows the calculated bandgap energies of $Ga_{0.97-y}Mn_{0.3}Cr_yAs$ together with experimental results. The $V_{Mn/Cr-VB}$ parameter used to fit the experimental results is 0.7 eV. As seen from Figure 3, the optical transition energies between CB and VB (red-circle in Figure 4), and CB and SO (triangle in Figure 4) bands increase with Cr composition, but the optical transition energy between IB of Mn (square in Figure 3) decreases with Cr as expected [15].

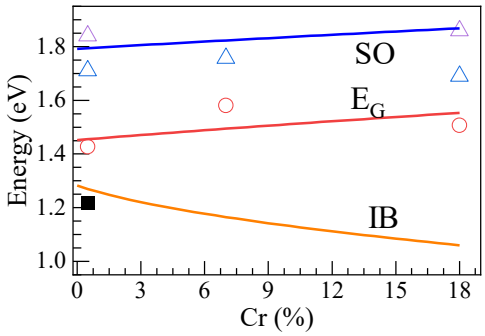

Figure 3: Calculated optical transition energies in all samples. Symbols and lines represent experimental and calculated optical transition energies, respectively. IB, E_G, and SO are impurity bandgap, fundamental bandgap, and spin split-off band edge, respectively.

Compering the T values in Table 2, the T_2 is attributed to the bandgap of $Ga_{0.97-y}Mn_{0.3}Cr_yAs$ alloys. The higher T_3 is attributed to CB-SO optical transitions. The lower transition energy in T_3 for the sample with 0.5 and 18% Cr may be originated from the localized states in the band edge as measured in GaAs layers.

CONCLUSIONS

The electronic band structure of $Ga_{1-x-y}Mn_xCr_yAs$ alloys was investigated by PR spectroscopy. PR signal was analyzed with TDFF signal form. All optical transition energies in $Ga_{0.97-y}Mn_{0.3}Cr_yAs$ layer increased with Cr atoms incorporated in the GaAs host lattice. The electronic band structure of $Ga_{0.97-y}Mn_{0.3}Cr_yAs$ alloys and the increment in optical transition energies were determined and accounted for by using the VBAC model, respectively. Comparing the optical transition in PR with VBAC model, the optical transitions are found to be between IB and CB, VB-CB and CB-SO bands.

ACKNOWLEDGEMENTS

This study was supported by the Scientific Research Projects Coordination Unit of Istanbul University (Project No: FDK-2019-35447, FDP-2020-36589 and FBG-2022-38573). We acknowledge Prof Hiroyuki AKINAGA for supplying the samples.

REFERENCES

[1] C. Caetano, R.R. Pela, S. Martini, M. Marques, L.K. Teles, Ab initio predictions of the stability and structural properties of zincblende (III,TM)V magnetic semiconductor alloys, J. Magn. Magn. Mater. 405 (2016) 274–281. https://doi.org/10.1016/j.jmmm.2016.01.011.

[2] T. Jungwirth, J. Wunderlich, V. Novák, K. Olejník, B.L. Gallagher, R.P. Campion, K.W. Edmonds, A.W. Rushforth, A.J. Ferguson, P. Němec, Spin-dependent phenomena and device concepts explored in (Ga,Mn)As, Rev. Mod. Phys. 86 (2014) 855–896. https://doi.org/10.1103/RevModPhys.86.855.

[3] L. Chioncel, I. Leonov, H. Allmaier, F. Beiuşeanu, E. Arrigoni, T. Jurcuţ, W. Pötz, Electronic correlations in short-period (CrAs)n/(GaAs) n ferromagnetic heterostructures, Phys. Rev. B - Condens. Matter Mater. Phys. 83 (2011) 1–9. https://doi.org/10.1103/PhysRevB.83.035307.

[4] M. Hashimoto, Y.-K. Zhou, M. Kanamura, H. Asahi, High temperature (>400 K) ferromagnetism in III–V-based diluted magnetic semiconductor GaCrN grown by ECR molecular-beam epitaxy, Solid State Commun. 122 (2002) 37–39. https://doi.org/10.1016/S0038-1098(02)00073-X.

[5] L. Lutz-Kappelman, Y. Zhang, G.J. Miller, Magnetic ordering and metal-atom site preference in tetragonal CrMnAs: Electronic correlation effects, J. Comput. Chem. 39 (2018) 1585–1593. https://doi.org/10.1002/jcc.25230.

[6] S. Choi, S.-K. Bac, X. Liu, S. Lee, S. Dong, M. Dobrowolska, J.K. Furdyna, Exchange bias in ferromagnetic bilayers with orthogonal anisotropies: the case of GaMnAsP/GaMnAs combination, Sci. Rep. 9 (2019) 13061. https://doi.org/10.1038/s41598-019-49492-4.

[7] H. Munekata, A. Zaslavsky, P. Fumagalli, R.J. Gambino, Preparation of (In,Mn)As/(Ga,Al)Sb magnetic semiconductor heterostructures and their ferromagnetic characteristics, Appl. Phys. Lett. 63 (1993) 2929–2931. https://doi.org/10.1063/1.110276.

[8] A. del Rio-de Santiago, C.F. Sánchez-Valdés, J.L. Sánchez Llamazares, M.A. Vidal, V.H. Méndez-García, M. López-López, E. Cruz-Hernández, Magnetic properties of GaAs:Mn self-assembled nanostructures grown at relatively high-temperature by Molecular Beam Epitaxy, J. Magn. Magn. Mater. 475 (2019) 715–720. https://doi.org/10.1016/j.jmmm.2018.12.030.

[9] K. Tivakornsasithorn, T. Yoo, H. Lee, S. Lee, S. Choi, S.K. Bac, K.J. Lee, S. Lee, X. Liu, M. Dobrowolska, J.K. Furdyna, Magnetization reversal and interlayer exchange coupling in ferromagnetic metal/semiconductor Fe/GaMnAs hybrid bilayers, Sci. Rep. 8 (2018) 1–11. https://doi.org/10.1038/s41598-018-28882-0.

[10] N.S. Al-Shameri, H. Dakhlaoui, Numerical investigation of quantum tunneling time and spin-current density in GaAs/GaMnAs/GaAs barriers: Role of an applied bias voltage, Phys. B Condens. Matter. 628 (2022) 413555. https://doi.org/10.1016/j.physb.2021.413555.

[11] Q. Wu, Y. Liu, H. Wang, Y. Li, W. Huang, J. Zhao, Y. Chen, Observation of spin-polarized photoconductivity in (Ga,Mn)As/GaAs heterojunction without magnetic field, Sci. Rep. 7 (2017) 1–8. https://doi.org/10.1038/srep40558.

[12] F. Yu, P.B. Parchinskiy, D. Kim, H. Kim, Y.E. Ihm, D.K. Choi, Effect of Be codoping on the photoluminescence spectra of GaMnAs, Curr. Appl. Phys. 11 (2011) 735–739. https://doi.org/10.1016/j.cap.2010.11.049.

[13] C. Caetano, L.K. Teles, M. Marques, L.G. Ferreira, Biaxial strain-induced suppression of spinodal decomposition in GaMnAs and GaCrAs, J. Appl. Phys. 107 (2010).

https://doi.org/10.1063/1.3448025.
[14] O. Yastrubchak, J. Żuk, H. Krzyżanowska, J.Z. Domagala, T. Andrearczyk, J. Sadowski, T. Wosinski, Photoreflectance study of the fundamental optical properties of (Ga,Mn)As epitaxial films, Phys. Rev. B. 83 (2011) 245201. https://doi.org/10.1103/PhysRevB.83.245201.
[15] K. Alberi, K.M. Yu, P.R. Stone, O.D. Dubon, W. Walukiewicz, T. Wojtowicz, X. Liu, J.K. Furdyna, Formation of Mn-derived impurity band in III-Mn-V alloys by valence band anticrossing, Phys. Rev. B. 78 (2008) 075201. https://doi.org/10.1103/PhysRevB.78.075201.
[16] H. Wu, H.D. Gan, H.Z. Zheng, J. Lu, H. Zhu, Y. Ji, G.R. Li, J.H. Zhao, Ferromagnetic nature of (Ga, Cr)As epilayers revealed by magnetic circular dichroism, Solid State Commun. 151 (2011) 456–459. https://doi.org/10.1016/j.ssc.2010.12.037.
[17] H. Saito, W. Zaets, R. Akimoto, K. Ando, Y. Mishima, M. Tanaka, Magnetic and transport properties of III–V diluted magnetic semiconductor Ga1−xCrxAs, J. Appl. Phys. 89 (2001) 7392–7394. https://doi.org/10.1063/1.1359475.
[18] L. Lutz-Kappelman, Y. Zhang, G.J. Miller, Magnetic ordering and metal-atom site preference in tetragonal CrMnAs: Electronic correlation effects, J. Comput. Chem. 39 (2018) 1585–1593. https://doi.org/10.1002/jcc.25230.
[19] X.Y. Cui, D. Fernandez-Hevia, B. Delley, A.J. Freeman, C. Stampfl, Embedded clustering in Cr-doped AlN: Evidence for general behavior in dilute magnetic III-nitride semiconductors, J. Appl. Phys. 101 (2007) 103917. https://doi.org/10.1063/1.2735405.
[20] M. Marques, L.G. Ferreira, L.K. Teles, L.M.R. Scolfaro, J. Furthmüller, F. Bechstedt, Magnetic properties of GaN/MnxGa1−xN digital heterostructures: First-principles and Monte Carlo calculations, Phys. Rev. B. 73 (2006) 224409. https://doi.org/10.1103/PhysRevB.73.224409.
[21] T. Dietl, Origin and control of ferromagnetism in dilute magnetic semiconductors and oxides (invited), J. Appl. Phys. 103 (2008) 07D111. https://doi.org/10.1063/1.2832613.
[22] K. Sato, H. Katayama-Yoshida, Design of Colossal Solubility of Magnetic Impurities for Semiconductor Spintronics by the Co-doping Method, Jpn. J. Appl. Phys. 46 (2007) L1120–L1122. https://doi.org/10.1143/JJAP.46.L1120.
[23] A. Bonanni, A. Navarro-Quezada, T. Li, M. Wegscheider, Z. Matěj, V. Holý, R.T. Lechner, G. Bauer, M. Rovezzi, F. D'Acapito, M. Kiecana, M. Sawicki, T. Dietl, Controlled Aggregation of Magnetic Ions in a Semiconductor: An Experimental Demonstration, Phys. Rev. Lett. 101 (2008) 135502. https://doi.org/10.1103/PhysRevLett.101.135502.
[24] P. Mahadevan, J.M. Osorio-Guillén, A. Zunger, Origin of transition metal clustering tendencies in GaAs based dilute magnetic semiconductors, Appl. Phys. Lett. 86 (2005) 172504. https://doi.org/10.1063/1.1921359.
[25] M. Gunes, O. Donmez, C. Gumus, A. Erol, H. Alghamdi, S. Alhassan, A. Alhassni, S. Alotaibi, M. Schmidbauer, H.V.A. Galeti, M. Henini, The effect of strain and spatial Bi distribution on the band alignment of GaAsBi single quantum well structure, Phys. B Condens. Matter. 602 (2021) 412487. https://doi.org/10.1016/j.physb.2020.412487.
[26] M. Gunes, M.O. Ukelge, O. Donmez, A. Erol, C. Gumus, H. Alghamdi, H.V.A. Galeti, M. Henini, M. Schmidbauer, J. Hilska, J. Puustinen, M. Guina, Optical properties of GaAs1-xBix/GaAs quantum well structures grown by molecular beam epitaxy on (100) and (311)B GaAs substrates, Semicond. Sci. Technol. 33 (2018) 124015. https://doi.org/10.1088/1361-6641/aaea2e.
[27] O. Donmez, A. Erol, M.C. Arikan, H. Makhloufi, A. Arnoult, C. Fontaine, Optical properties of GaBiAs single quantum well structures grown by MBE, Semicond. Sci. Technol. 30 (2015). https://doi.org/10.1088/0268-1242/30/9/094016.
[28] D.E. Aspnes, Third derivative modulation spectroscopy theory with low-field electroreflectance, Surf. Sci. 37 (1973) 418.
[29] T.J.C. Hosea, Estimating critical point parameters of modulated reflectance spectra, Phys. Status Solidi B. 189 (1995) 531.
[30] O. Donmez, F. Nutku, A. Erol, C.M. Arikan, Y. Ergun, A study of photomodulated reflectance on staircase-like, n-doped GaAs/AlxGa1-xAs quantum well structures., Nanoscale Res. Lett. 7 (2012)

622. https://doi.org/10.1186/1556-276X-7-622.
[31] O. Donmez, A. Erol, M.C. Arikan, H. Makhloufi, A. Arnoult, C. Fontaine, Optical properties of GaBiAs single quantum well structures grown by MBE, Semicond. Sci. Technol. 30 (2015) 094016. https://doi.org/10.1088/0268-1242/30/9/094016.
[32] O. Donmez, A. Erol, Investigating above-bandgap and below-bandgap optical transition in GaBiAs epilayers by photoreflectance spectroscopy, Turkish J. Phys. 44 (2020) 384–393. https://doi.org/10.3906/fiz-2003-17.
[33] J. Misiewicz, R. Kudrawiec, Contactless electroreflectance spectroscopy of optical transitions in low dimensional semiconductor structures, Opto-Electronics Rev. 20 (2012) 101–119. https://doi.org/10.2478/s11772-012-0022-1.
[34] B.C. Chapler, R.C. Myers, S. Mack, A. Frenzel, B.C. Pursley, K.S. Burch, E.J. Singley, A.M. Dattelbaum, N. Samarth, D.D. Awschalom, D.N. Basov, Infrared probe of the insulator-to-metal transition in Ga1-xMnxAs and Ga1-xBexAs, Phys. Rev. B. 84 (2011) 081203. https://doi.org/10.1103/PhysRevB.84.081203.
[35] R.R. Pelá, M. Marques, L.G. Ferreira, J. Furthmüller, L.K. Teles, GaMnAs: Position of Mn- d levels and majority spin band gap predicted from GGA-1/2 calculations, Appl. Phys. Lett. 100 (2012) 202408. https://doi.org/10.1063/1.4718602.
[36] A.M. Hennel, Transition Metals in III/V Compounds, in: Semicond. Semimet., 1993: pp. 189–234. https://doi.org/10.1016/S0080-8784(08)62801-X.